Dynamic Fast-Acquisition ECE Diagnostic for Turbulence Studies in TCV

J. W. Tumbokon, S. Coda, L. Porte and the TCV team*

Ecole Polytechnique Fédérale de Lausanne (EPFL), Swiss Plasma Center (SPC), CH-1015 Lausanne, Switzerland

** See the author list of C. Theiler et al. 2026 Nucl. Fusion 66 116007*

Introduction

The interplay between magnetohydrodynamic (MHD) instabilities and turbulence in fusion plasmas is not well understood [1]. Reduced MHD models [2] and gyrokinetic simulations [3] suggest that MHD instabilities are driven and amplified by turbulence, but experimental demonstrations remain a difficulty due to limitations in hardware and the elusiveness of the predicted causal relation. In magnetic confinement devices, plasma diagnostics are used, among other things, to characterise turbulent structures in plasmas through measurements of density and/or temperature fluctuations. In particular, microwave diagnostics such as the Electron Cyclotron Emission (ECE) will be one of the few diagnostic techniques that can be operated in future fusion devices at a high neutron fluence [4]. ECE diagnostics in TCV [5] are able to capture a broad range of electron temperature fluctuations, from magnetohydrodynamic (MHD) instabilities (<50 kHz) to turbulent flows (~10s to 100s of kHz), with high spatial (~1 cm) and temporal (~1 μs) resolution along a 1D horizontal line-of-sight. In this work, we briefly describe a new, dynamic method of acquiring ECE data in TCV, comparing it with the current setup, and discussing its main strength as a secondary diagnostic.

Fast-acquisition ECE & digital radiometry

ECE is a passive diagnostic. Signals are obtained by receiving radiation emitted by electrons gyrating along field lines (Fig. 1(a)). In TCV, second-harmonic electron cyclotron emission is observed in the radiofrequency (RF) range (~60-100 GHz). Heterodyne radiometry is used to detect these RF emissions, which are first downconverted to intermediate frequencies (IF, 2-20 GHz), then divided into frequency bands, and finally low-pass filtered into acquisition (Fig. 1(b)).

The fast-acquisition method relies heavily on a 32 GS/s Analog-to-Digital Converter (ADC) to fully digitise IF signals after downconversion. This method has been previously applied on TEXTOR [6] and LHD [7], but the setup used here is simpler than the former (one ADC instead of four), with a larger time range than the latter (1.6 s instead of 6.4 ms). Here, the ADC has an analog bandwidth of 10 GHz, corresponding to a spatial range of radial temperature measurements

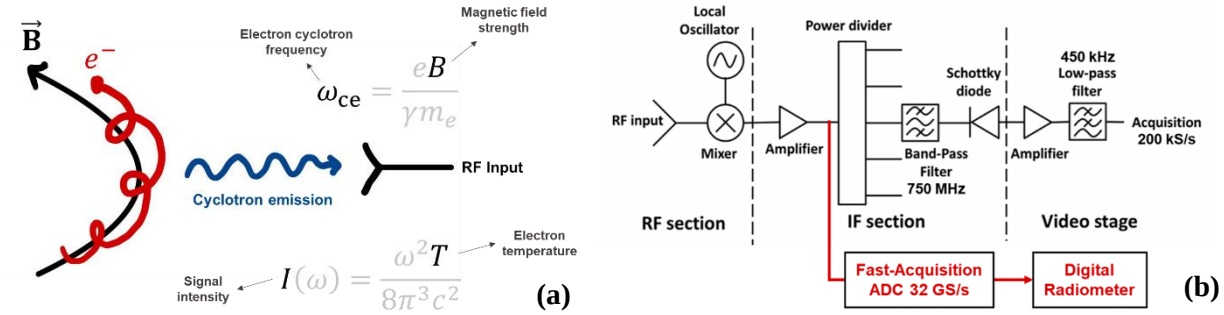

Figure 1: (a) Depiction of cyclotron emission detection. (b) Schematic of the ECE diagnostic in TCV, modified from [4]. The new method acquires the signal before the power divider using an ultra-fast sampling 32 GS/s ADC. The raw signal is then digitally processed into ECE signals.

$\rho_\psi \sim 0.7 - 1$ in TCV. In essence, IF signals are split into time segments, where the FFT spectrum of each segment is integrated over the desired bandpass window to give a power time series proportional to electron temperature. Digital ECE channels are dynamic; radial position and spatial resolution are changed by varying the central frequency and bandwidth of the integration window, while time resolution is changed by varying the number of data points in each time segment. The strength of this method lies in post-processing, where the same data can be processed with varying resolutions, without having to repeat experiments.

Benchmarking against the physical radiometer

The digitally-processed signals closely resemble those of the physical ECE radiometer. An example is shown in Fig. 2, where a digital ECE channel was configured to replicate one of the physical bandpass channels. The discrepancy is most likely attributed to a difference in the filter shapes; a physical bandpass filter deviates from a perfect Hann window, where the latter is used in digital processing.

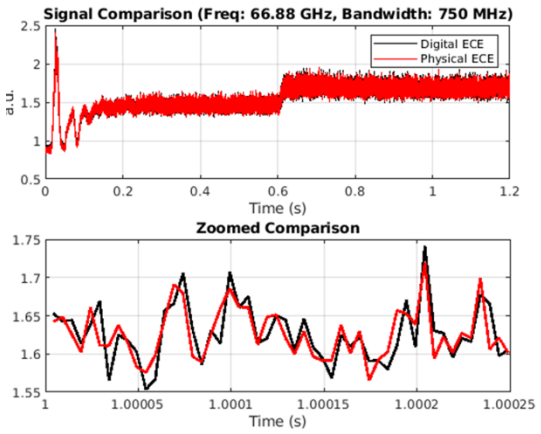

Figure 2: Comparison between physical (red) and digital (black) ECE signals.

Turbulence measurements with the digital radiometer

With the validated method, we configure the digital radiometer for turbulence measurements: a finer temporal resolution (1 us vs 5 us) and spatial resolution (500 MHz vs 750 MHz channel bandwidth). We choose a scenario with a Neoclassical Tearing Mode (NTM) induced by Electron Cyclotron Heating (ECH) to demonstrate its ability to detect both MHD and turbulence scale fluctuations. The cross-power spectral density (CPSD) plot (Fig. 3), calculated using Welch's method [8], between two digital ECE channels impressively characterises broadband turbulence up to 400 kHz, simultaneously resolving a 5 kHz NTM mode. Repeating this analysis for multiple radial locations in the plasma would provide spatially-resolved information on turbulence and MHD.

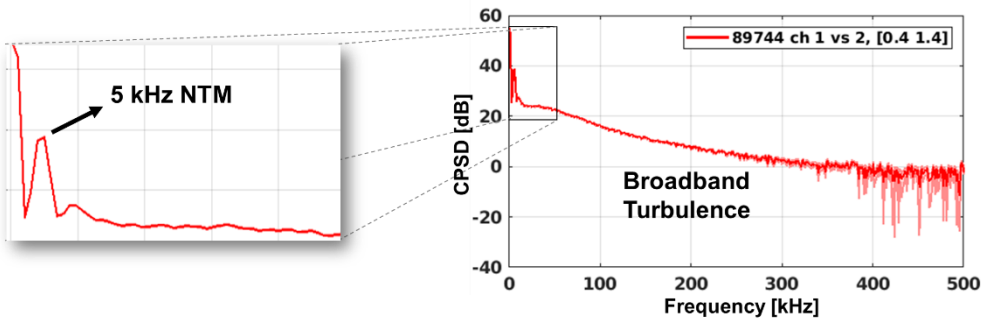

Figure 3: Cross-power spectral density (CPSD) between two digital ECE channels resolve a Neoclassical Tearing Mode (NTM) at 5 kHz and broadband turbulence up to 400 kHz.

To further demonstrate this method's ability to perform spatiotemporal turbulence measurements, we showcase a scenario where Neutral Beam Heating (NBH) power is varied throughout the experiment. Here, electron temperature fluctuations $\delta T_e/T_e$ are calculated from Eq. 1 in [9]. From Fig. 4, we observe heightened turbulence amplitudes towards the edge ($\rho_\psi \sim 0.95$) throughout the shot. Interestingly, the relative fluctuation level plot shows distinctive patterns between the three phases, where turbulent activity seems to shift towards the core. The reliability of this data is supported by the fact that all digital channels share the same gains, offsets, and window filter shape; it would be extremely difficult to achieve such a setup using physical filters. This justifies cross-channel comparisons.

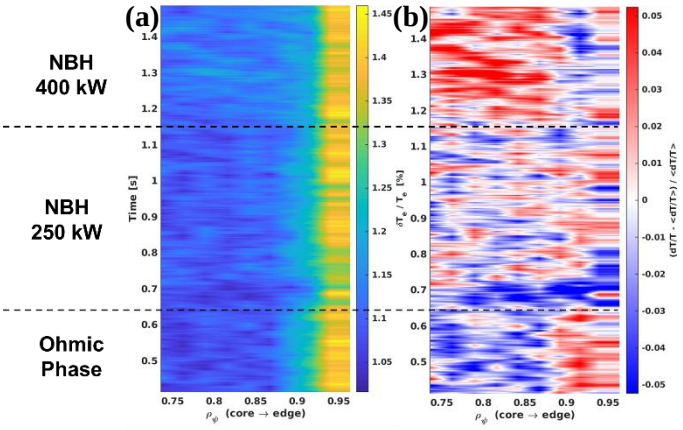

Figure 4: Hövmoller diagrams showing time on the vertical axis and radial position on the horizontal axis, where quantities are calculated from digital ECE channel data. (a) Complex turbulence amplitudes show elevated activity towards the edge. (b) Normalised relative fluctuation levels show varying turbulent activity between the three phases.

Limitations & Outlook

The main strength of fast-acquisition ECE lies in post-processing; once raw data is obtained, dynamic acquisition involving varying spatiotemporal resolution parameters can be indefinitely performed without the need to repeat an experiment. Additionally, the consistent filter shape results in less noise due to spectral leakage, and hence more reliable data. However, the main problem is that with such a high sampling rate, 1.6 s of raw data takes up 100 GB of storage space. With a fast computer and optimised algorithms, it would be possible to run a standard post-shot analysis where only the processed data is kept. In this case, the raw data will be deleted by default, with the option of keeping the raw data for particularly valuable shots. Otherwise, this technique will serve as a supporting diagnostic to be used alongside measurements from the physical radiometer, in cases where the enhanced resolution will greatly benefit the study. In other words, this method would only be used upon request. Topics of interest are the detection of smaller

magnetic islands (<2 cm) and the experimental detection of turbulence-driven magnetic islands (TDMI) [10].

Another constraint is that the 10 GHz ADC analog bandwidth imposes a limit on spatial range, where flux surfaces towards the core ($\rho_\psi < 0.7$) are out of reach. The plan for the future is to simultaneously use two ADC channels, where IF from the high-frequency side is inputted into the second channel. This would enable the digital radiometer to access the full range of flux surfaces, allowing the detection and study of MHD instabilities toward the magnetic axis, such as fishbones. It is noted that having two channels would double the amount of data per experiment, but once we are satisfied with the processed results, the raw data can always be deleted, save a few trophy shots.

References

[1] M. J. Choi et al. Nat. Commun. 12, 375 (2021)

[2] M. Muraglia et al. Phys. Rev. Lett. 107, 095003 (2011)

[3] W. A. Hornsby et al. Plasma Phys. Control. Fusion 58, 014028 (2016)

[4] A. Kohn-Seemann and R. B. Morales Phys. Plasmas 32, 060502 (2025)

[5] M. Fontana, PhD thesis, EPFL TH9016 (2018)

[6] W. A. Bongers et al. Rev. Sci. Instrum. 82, 063508 (2011)

[7] H. Tsuchiya et al. Plasma Fusion Res. 9, 3402021 (2014)

[8] P. D. Welch IEEE Trans. Audio Electroacoust. AU-15, 70 (1967)

[9] P. A. Molina Cabrera et al. Plasma Phys. Control. Fusion 65, 055010 (2023)

[10] O. Agullo et al. Phys. Plasmas 21 092303 (2014)